

Supplementary Information

Negative Thermal Expansion in $\text{Sc}_2\text{Mo}_3\text{O}_{12}:\text{Sm}^{3+}$ for White LEDs and Unveiling the Impact of Phase Transition on Cryogenic Luminescence

Annu Balhara,^{1,2} Santosh K. Gupta,^{1,2*} Malini Abraham,^{3,4} Ashok Kumar Yadav,⁵ Mohsin Jafar,⁶ Subrata Das,^{3,4}

¹Radiochemistry Division, Bhabha Atomic Research Centre, Trombay, Mumbai-400085, India

²Homi Bhabha National Institute, Mumbai-400094

³Materials Science and Technology Division, CSIR-National Institute for Interdisciplinary Science and Technology, Thiruvananthapuram, Kerala-695019

⁴Academy of Scientific and Innovative Research (AcSIR), Ghaziabad-201002, India

⁵Atomic & Molecular Physics Division, Bhabha Atomic Research Centre, Mumbai – 400085

⁶Chemistry Division, Bhabha Atomic Research Centre, Trombay, Mumbai-400085, India

**To whom correspondence should be addressed. Electronic mail: *santoshg@barc.gov.in/santufrnd@gmail.com (SKG)*

S1. Characterization

The powder XRD patterns were acquired on a Proto-AXRD bench top system in the 2θ range of $10-70^\circ$ using the Cu $K\alpha$ line ($\lambda = 1.5406 \text{ \AA}$) and a scanning rate of $1^\circ/\text{min}$. Fourier Transform Infrared Spectroscopy (FTIR) was performed in ATR mode on a Bruker Alpha FTIR spectrometer in the scanning range from 500 to 4000 cm^{-1} using average of 36 scans with a resolution of 4 cm^{-1} . The scanning electron microscopy (SEM) was performed on a SEM (Model: JEOL ICM6000Plus-7E, Japan) system at 15 kV. Rietveld refinement was done on powder XRD patterns by using FullProf software.¹ HT-XRD measurements were done on GNR Explore X-ray Diffractometer with a heating rate of 10 K/min and equilibrium time of 10 minutes. An X-ray Absorption Spectroscopy (XAS) measurement, which comprises of both X-ray Near Edge Structure (XANES) and Extended X-ray Absorption Fine Structure (EXAFS)

techniques, have been carried out on undoped and Sm doped $\text{Sc}_2\text{Mo}_3\text{O}_{12}$ at Mo K-edge in transmission mode and Sm L_3 -edge in fluorescence mode to probe the local structure. The XAS measurements have been carried out at the Energy-Scanning EXAFS beamline (BL-9) at the Indus-2 Synchrotron Source (2.5 GeV, 100 mA) at Raja Ramanna Centre for Advanced Technology (RRCAT), Indore, India.^{2, 3} PL and PLE spectra were recorded with a continuous Xenon lamp (450 W) source on a FLS 1000 fluorescence spectrometer (Edinburgh Instruments, U.K.), and visible-PMT as the detector. Emission photographs were captured under the excitation wavelength of 270 nm by Nikon camera. Low temperature-dependent PL studies were performed using cryostat assembly with FLS-1000 fluorescence spectrometer and liquid nitrogen as coolant. Temperature-dependent PL spectra at high temperature were measured using an Ocean optics spectrophotometer that has a Maya 2000 PRO with a 280 nm LEDs as excitation source. Differential scanning calorimeter (DSC) measurements were performed on M/s. Mettler Toledo GmbH, Switzerland. A prototype white-LED was fabricated by pasting a mixture of phosphors onto a 280 nm UV LED chip operating at a voltage of 12 V and current of 2 A. The red pc-LEDs were fabricated by combining this optimized red phosphor with a 280 nm UV-LED chip and a 410 nm blue LED chip individually, both operated at a voltage of 12 V and current of 2 A. The temperature-dependent Raman spectroscopy was performed using the Linkam thermal stage (HFS600E) having temperature control accuracy of 1 °C and a heating rate of 10 °C min⁻¹. A sufficient time hold of 5 min is taken at each temperature step for sample temperature stabilization.

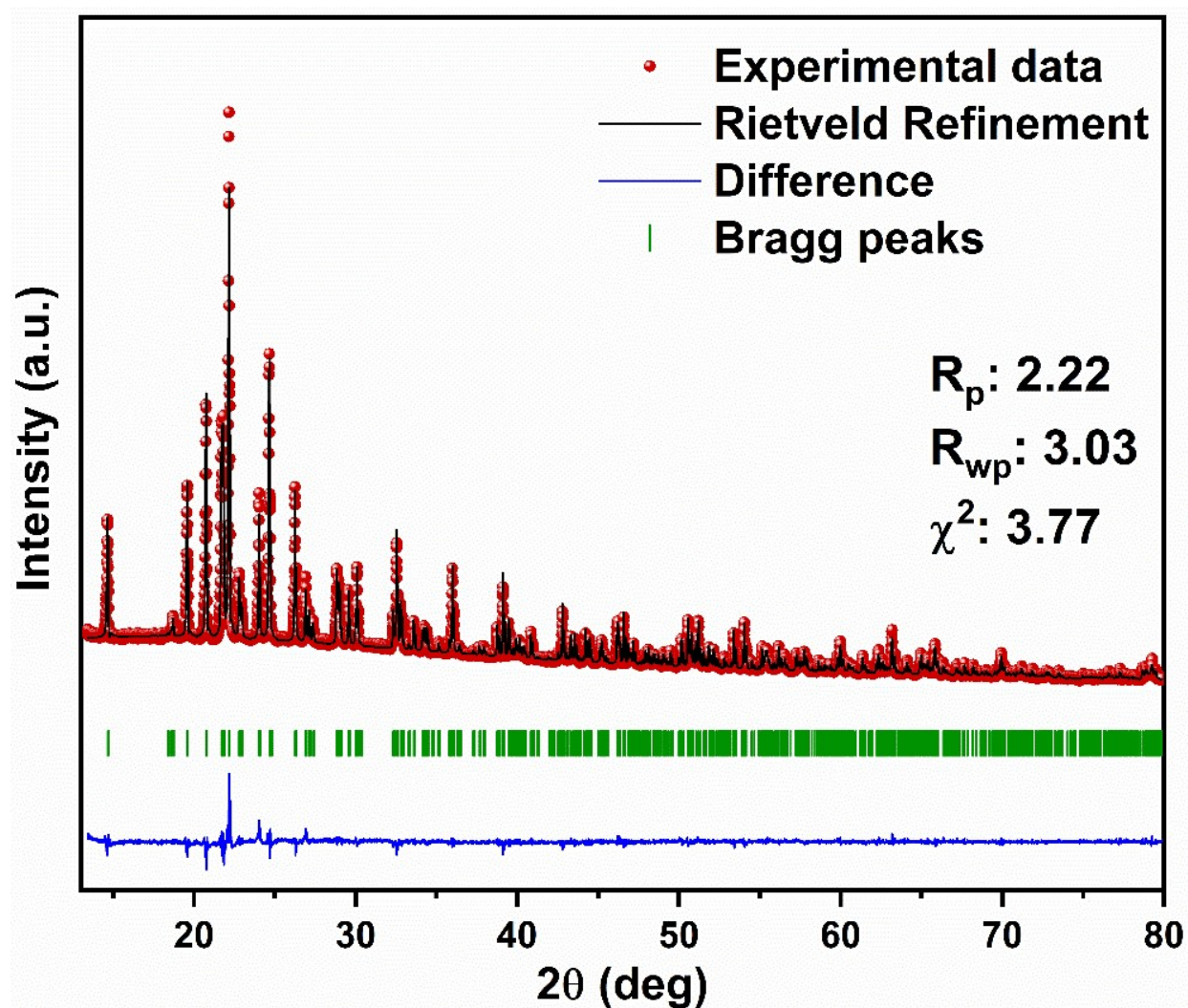


Figure S1: Rietveld fitting of powder XRD patterns of undoped $\text{Sc}_2\text{Mo}_3\text{O}_{12}$ sample at room temperature.

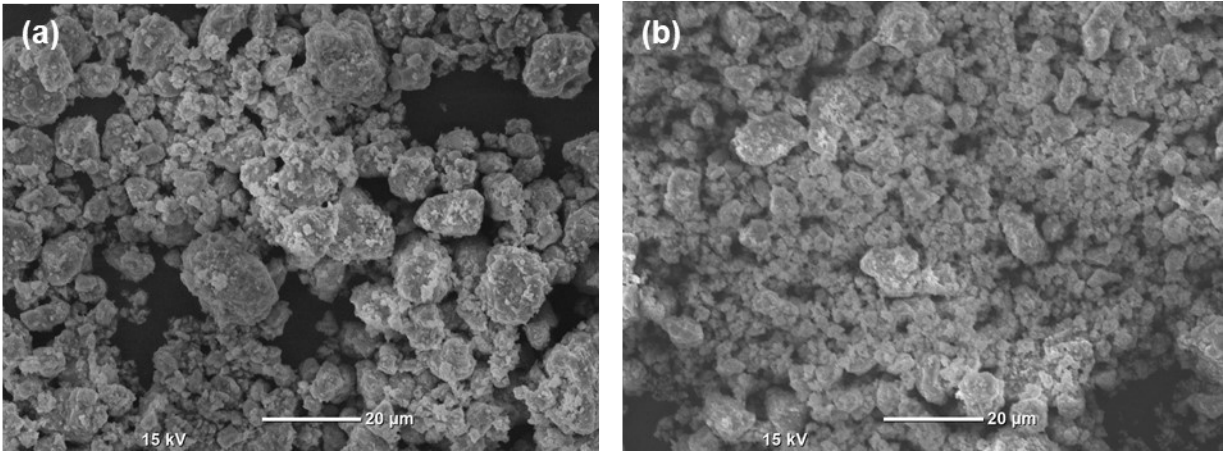


Figure S2: SEM images of (a) SMO:5Sm and (b) SMO:10 Sm phosphors.

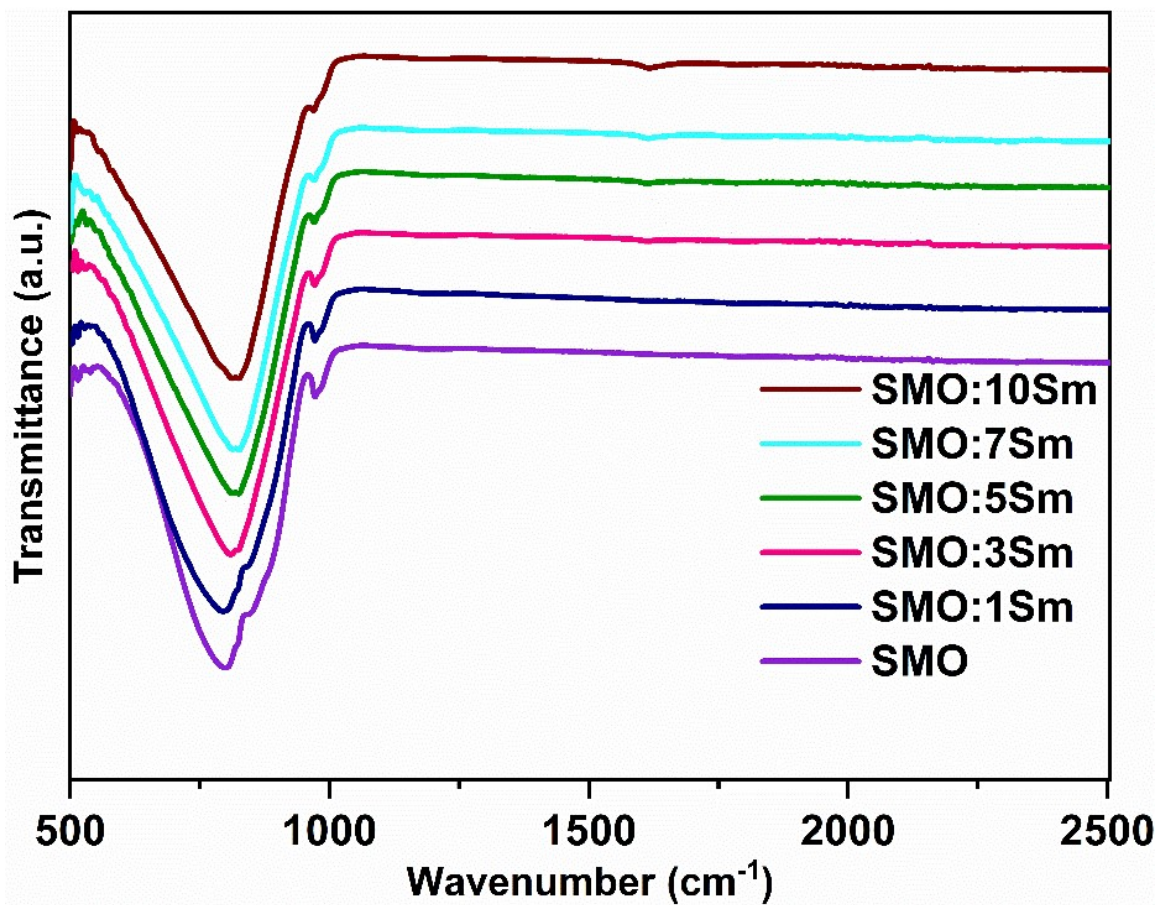


Figure S3: FTIR spectra of Sc₂Mo₃O₁₂:xSm³⁺ ($x = 0, 1, 3, 5, 7$ and 10 mol %) phosphors.

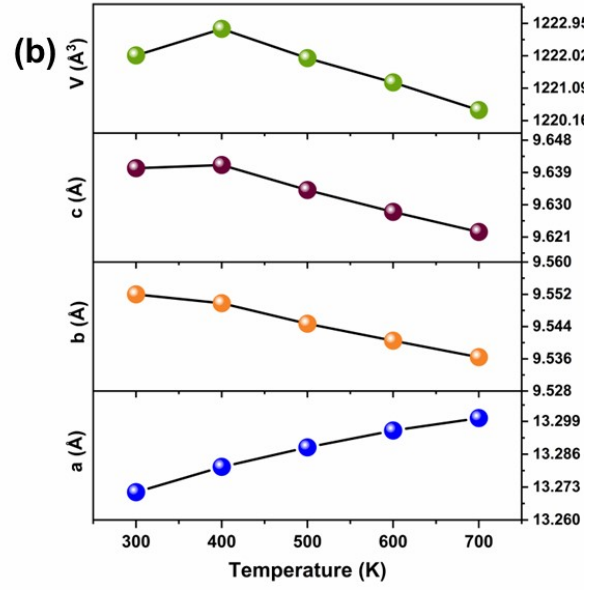
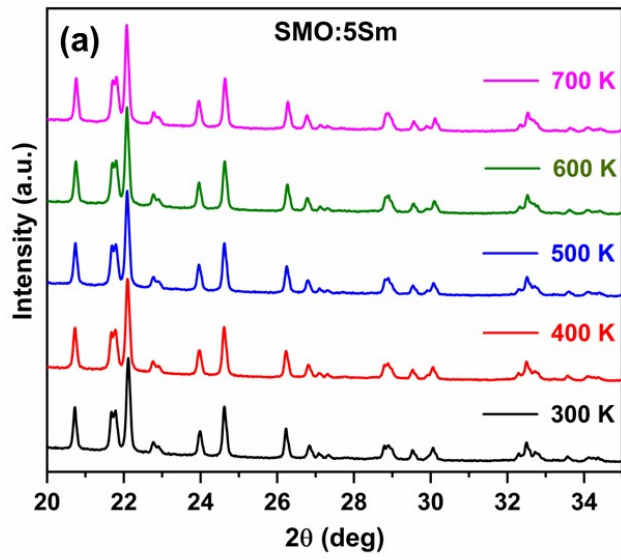


Figure S4: (a) High temperature-dependent XRD patterns of SMO:5Sm sample and (b) Changes in unit cell parameters with temperature in the range of 300 to 700 K.

Table S1: Lattice parameters for SMO at different temperature from 300 to 700 K

Temperature (K)	a (Å)	B (Å)	c (Å)	V (Å ³)
300	13.2403(3)	9.5426(3)	9.6356(3)	1217.425(045)
400	13.2516(9)	9.5345(9)	9.6282(9)	1216.511(180)
500	13.2615(9)	9.5292(9)	9.6201(9)	1215.720(180)
600	13.2698(15)	9.5244(9)	9.6129(12)	1214.941(240)
700	13.2770(15)	9.5216(9)	9.6071(12)	1214.510(240)

Table S2: Lattice parameters for SMO:5Sm at different temperature from 300 to 700 K.

Temperature (K)	a (Å)	B (Å)	c (Å)	V (Å ³)
300	13.2710(3)	9.5520(3)	9.6402(3)	1222.030(072)
400	13.2810(12)	9.5498(9)	9.6411(9)	1222.793(210)
500	13.2887(12)	9.5447(9)	9.6341(9)	1221.953(210)
600	13.2954(6)	9.5405(6)	9.6280(6)	1221.256(105)
700	13.3003(12)	9.5364(9)	9.6224(9)	1220.461(180)

Table S3: Lifetime values of SMO:Sm samples at 647 nm emission and $\lambda_{\text{ex}} = 270$ nm and 404 nm, respectively.

$\lambda_{\text{ex}} = 270$ nm and $\lambda_{\text{em}} = 647$ nm					
Sample	τ_1 (μs)	%	τ_2 (μs)	%	τ_{av} (μs)
1Sm	452 \pm 10.1	17.49	1143.5 \pm 4.60	82.51	1022.56 \pm 4.19
3Sm	364 \pm 3.61	35.8	1020 \pm 4.27	64.2	785.15 \pm 3.03
5Sm	298.5 \pm 2.81	41.6	952.8 \pm 4.82	58.4	680.61 \pm 3.04
7Sm	274 \pm 2.45	43.63	896.05 \pm 4.81	56.37	624.65 \pm 2.91
10Sm	271 \pm 2.21	47.71	892.92 \pm 4.89	52.29	596.20 \pm 2.77
$\lambda_{\text{ex}} = 404$ nm and $\lambda_{\text{em}} = 647$ nm					
Sample	τ_1 (μs)	%	τ_2 (μs)	%	τ_{av} (μs)
1Sm	387 \pm 8.16	16.99	1110 \pm 3.94	83.01	987.16 \pm 3.55
3Sm	303.8 \pm 3.84	32.14	905.94 \pm 4.26	67.86	712.41 \pm 3.14
5Sm	253.1 \pm 3.24	39.65	793.33 \pm 5.10	60.35	579.13 \pm 3.33
7Sm	255.86 \pm 2.99	43.7	773.5 \pm 5.28	56.31	547.37 \pm 3.25
10Sm	220.34 \pm 2.29	43.72	714.41 \pm 4.29	56.28	498.40 \pm 2.62

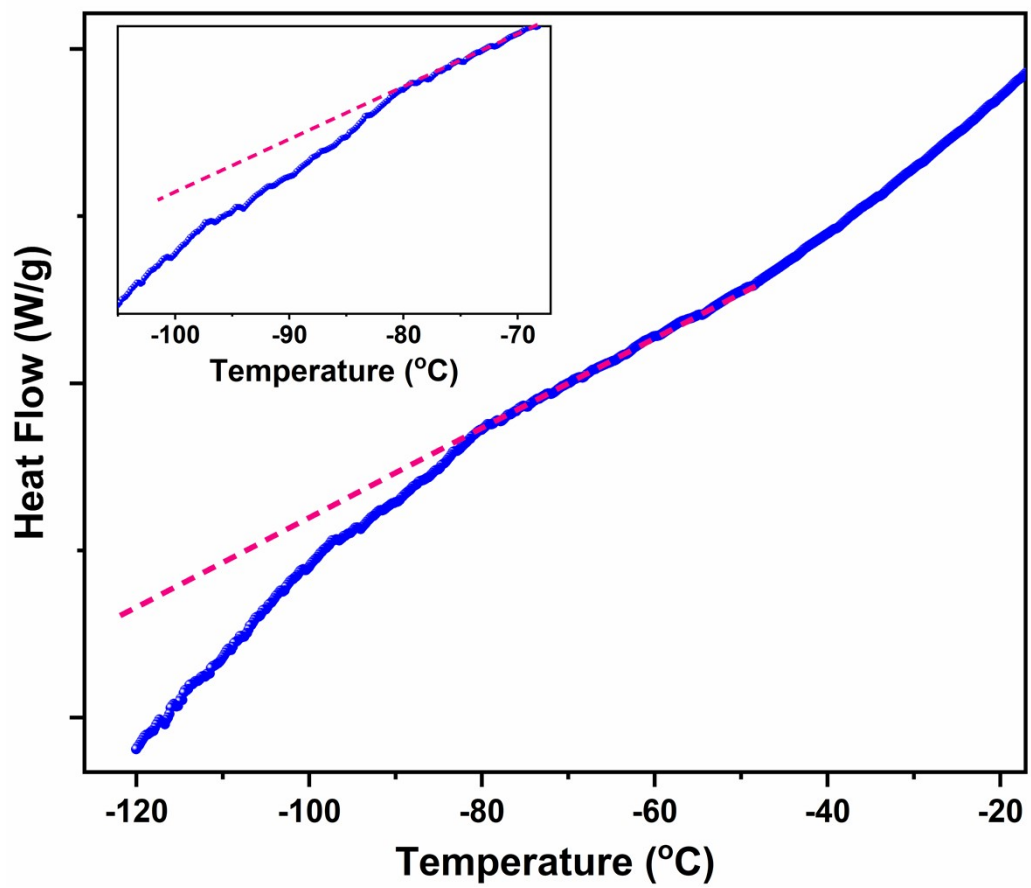


Figure S5: DSC Curve showing the phase transition.

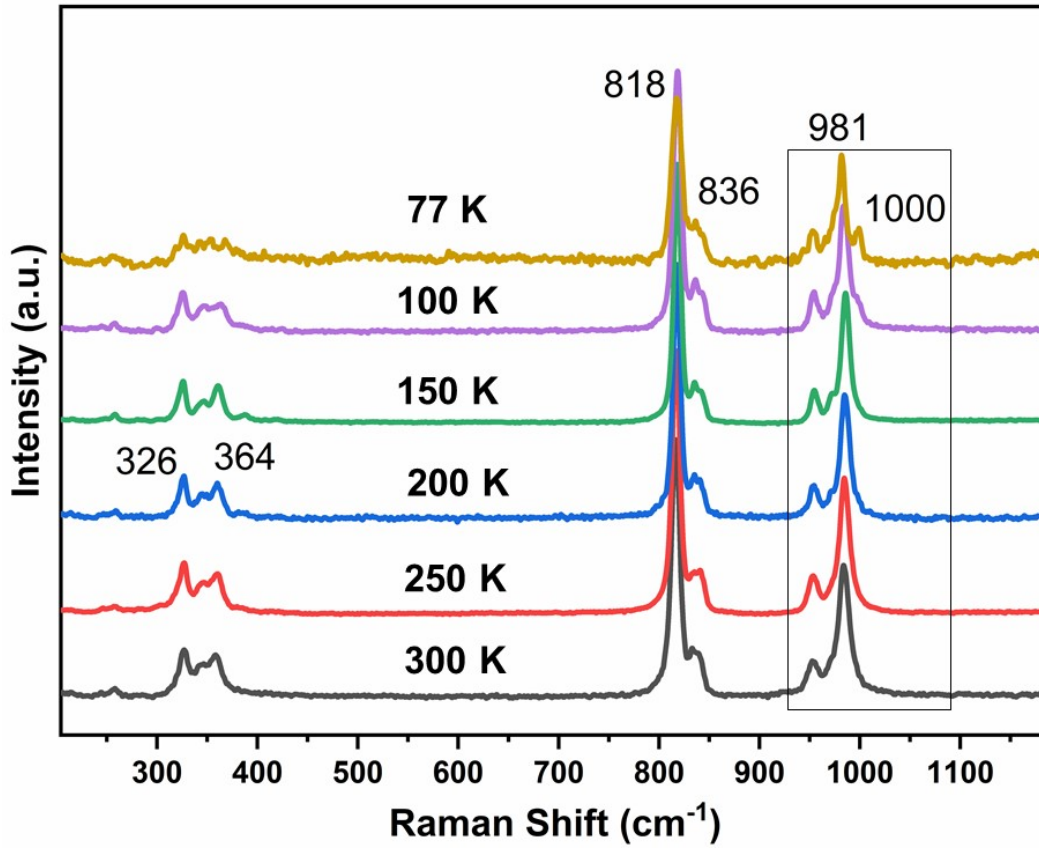


Figure S6: Raman spectra of Sc₂Mo₃O₁₂:5Sm at different temperatures.

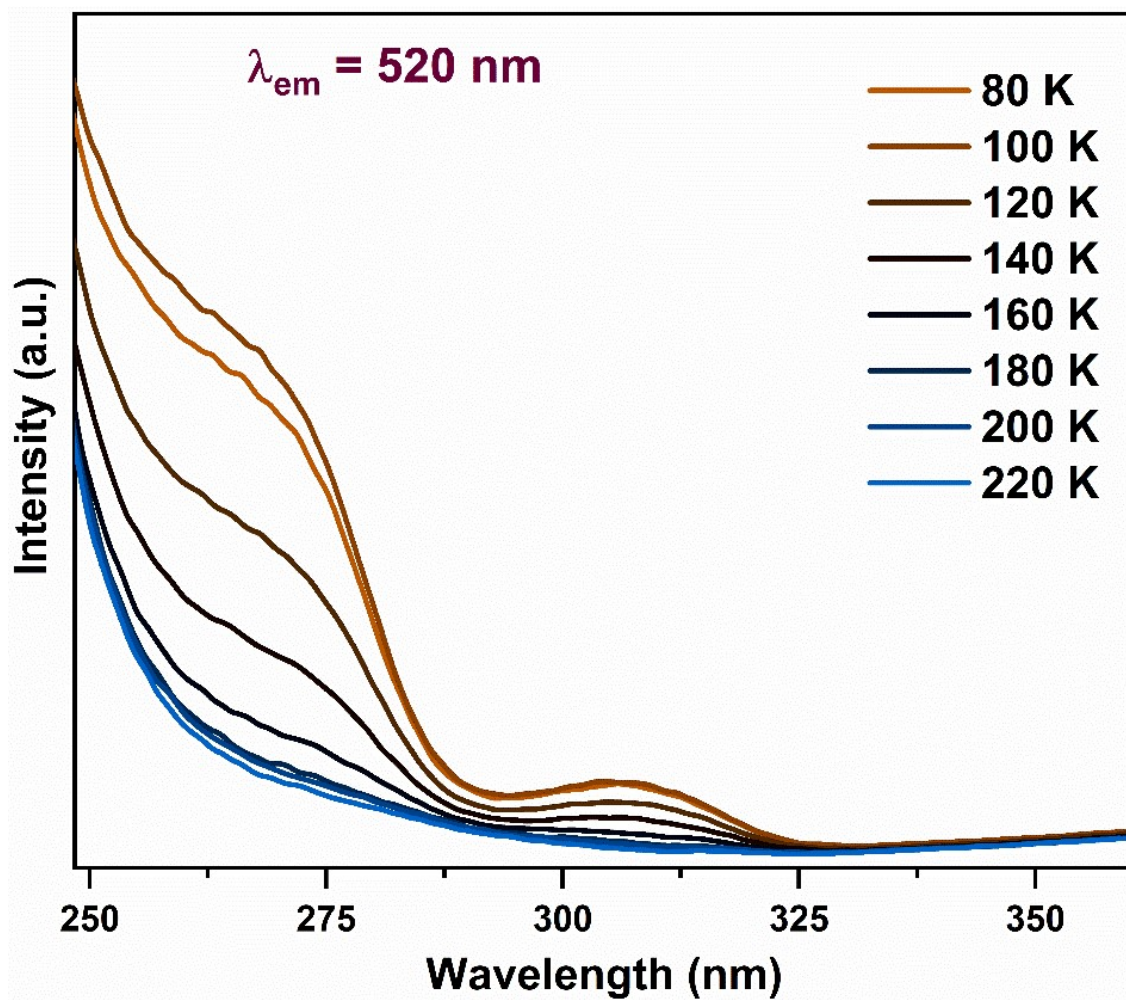


Figure S7: Temperature-dependent PL excitation spectra of SMO:5Sm sample monitored at 520 nm emission in the range of 80 to 300 K.

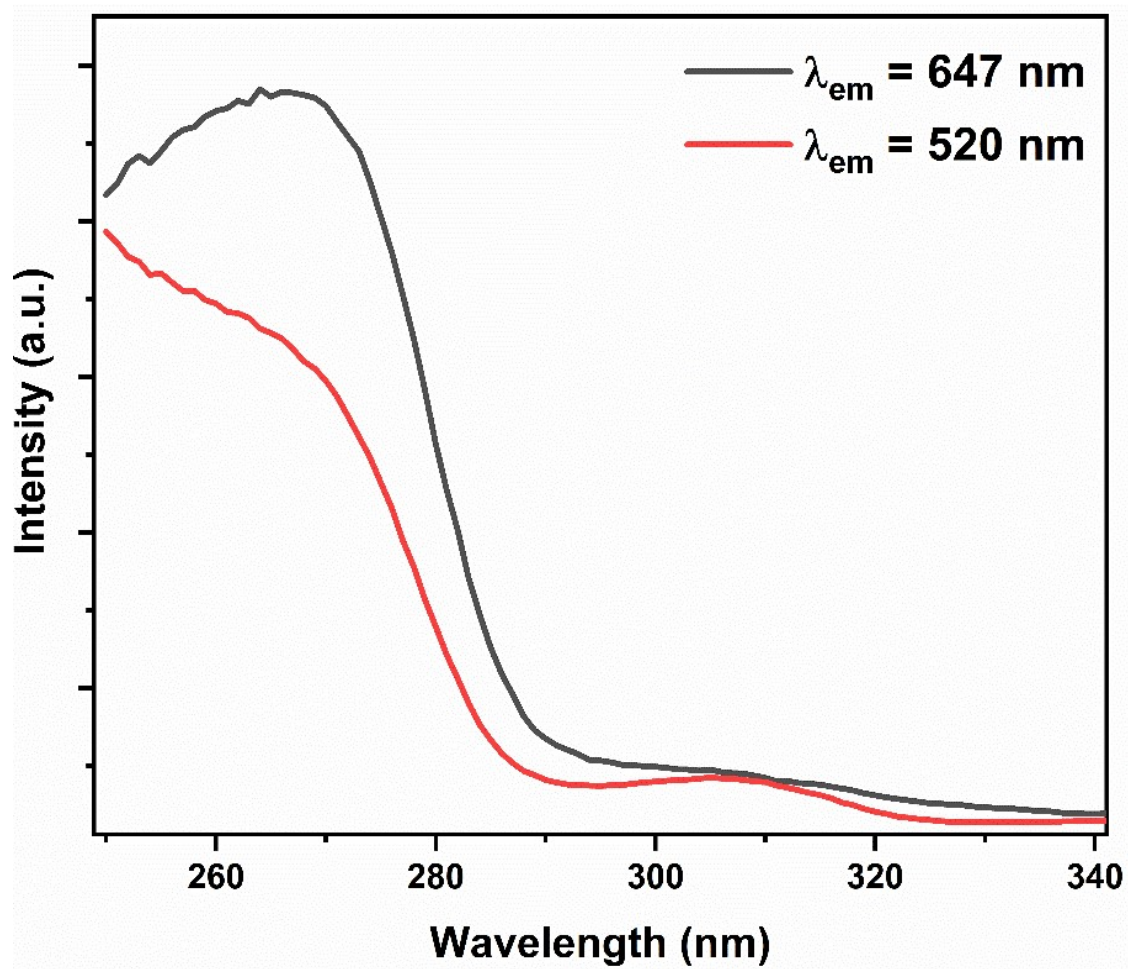


Figure S8: Excitation spectrum acquired at host emission (520 nm) and Sm^{3+} emission (647 nm).

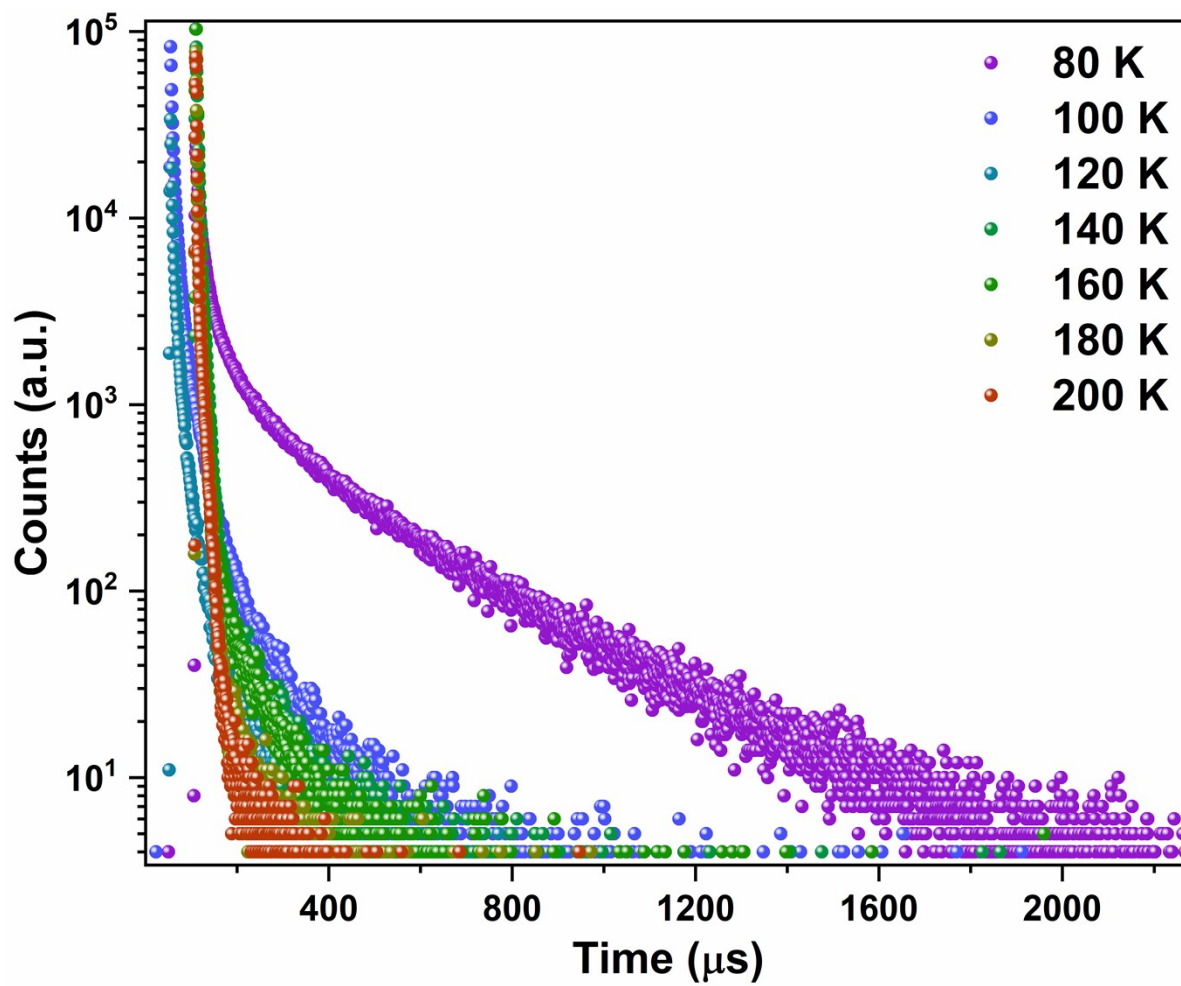


Figure S9: Temperature-dependent decay profiles of SMO:5Sm sample for 520 nm emission excited at 270 nm.

Table S4: Temperature-dependent Lifetime values of SMO:Sm samples at 647 nm emission and $\lambda_{\text{ex}} = 270$ nm from 80 to 300 K.

T (K)	τ_1 (μs)	%	τ_2 (μs)	%	τ_{av} (μs)
80	237.43 \pm 4.80	24.7	1382.14 \pm 10.87	75.3	1099.40 \pm 8.27
100	244.7 \pm 11.61	18.4	1380.9 \pm 15.95	81.6	1171.84 \pm 13.19
120	305.9 \pm 8.22	20.7	1410.3 \pm 12.29	79.3	1181.69 \pm 9.89
140	272.63 \pm 8.75	22.3	1380.6 \pm 14.40	77.7	1133.52 \pm 11.36
160	232.36 \pm 7.00	23.2	1288.2 \pm 12.89	76.8	1043.24 \pm 10.03
180	245.71 \pm 6.30	27.2	1296.89 \pm 13.27	72.8	1010.97 \pm 9.81
200	228.46 \pm 6.14	25.4	1224.36 \pm 11.75	74.6	971.20 \pm 8.90
220	223.4 \pm 5.43	28.6	1218.65 \pm 12.17	71.4	934.01 \pm 8.83
240	243.75 \pm 6.06	30.1	1209.46 \pm 13.15	69.9	918.78 \pm 9.37
260	250.37 \pm 5.30	33.3	1249.46 \pm 13.19	66.8	917.26 \pm 8.98
280	216.2 \pm 4.16	32.1	1113.67 \pm 9.60	67.9	825.58 \pm 6.66
300	177.02 \pm 3.98	34.6	687.13 \pm 7.37	65.4	510.63 \pm 5.01

Table S5: Temperature-dependent Lifetime values of SMO:Sm samples at 647 nm emission and $\lambda_{\text{ex}} = 404$ nm from 80 to 300 K.

T (K)	τ_1 (μs)	%	τ_2 (μs)	%	τ_{av} (μs)
80	222 \pm 16.53	19.2	1183.6 \pm 29.13	80.8	998.97 \pm 23.75
100	207 \pm 15.76	18.5	1118.5 \pm 25.94	81.5	949.87 \pm 21.34
120	266.03 \pm 17.82	24.4	1135.12 \pm 28.54	75.6	923.06 \pm 22.01
140	169.42 \pm 11.36	19.0	1030.1 \pm 20.78	81.0	866.66 \pm 16.97
160	239.5 \pm 8.62	27.6	1199.4 \pm 20.52	72.4	934.47 \pm 15.05
180	188.67 \pm 14.27	19.8	998.99 \pm 25.49	80.2	838.55 \pm 20.64
200	163.65 \pm 9.80	20.7	954.3 \pm 18.46	79.3	790.63 \pm 14.78

220	184.95 ± 10.69	23.2	975.28 ± 21.24	76.8	791.92 ± 16.50
240	204.6 ± 11.27	27.5	1007 ± 26.17	72.5	786.34 ± 19.22
260	204.1 ± 10.56	28.4	1014.3 ± 26.97	71.6	784.20 ± 19.54
280	206.15 ± 11.01	32.4	883.8 ± 30.63	67.6	664.24 ± 21.01
300	170.4 ± 10.52	30.7	661.5 ± 21.42	69.3	510.73 ± 15.19

References

1. Rodríguez-Carvajal, J., Recent advances in magnetic structure determination by neutron powder diffraction. *Physica B: Condensed Matter* 1993, 192, (1), 55-69.
2. Basu, S.; Nayak, C.; Yadav, A.; Agrawal, A.; Poswal, A.; Bhattacharyya, D.; Jha, S.; Sahoo, N. In *A comprehensive facility for EXAFS measurements at the INDUS-2 synchrotron source at RRCAT, Indore, India*, Journal of Physics: Conference Series, 2014; IOP Publishing: 2014; p 012032.
3. Poswal, A.; Agrawal, A.; Yadav, A.; Nayak, C.; Basu, S.; Kane, S.; Garg, C.; Bhattacharyya, D.; Jha, S.; Sahoo, N. In *Commissioning and first results of scanning type EXAFS beamline (BL-09) at INDUS-2 synchrotron source*, AIP Conference Proceedings, 2014; American Institute of Physics: 2014; pp 649-651.